



Synthesis, characterization and molecular docking studies of novel Schiff bases bearing 1-(*o*-tolyl)-4-(phenoxyethyl)-(1*H*)1,2,3-triazole derivatives

Selbi KESKİN^{1*}, Derya VURAL²

¹Department of Chemistry, Faculty of Arts and Sciences, Giresun University, 28200, Giresun, Türkiye

²Department of Physics, Faculty of Science, Marmara University, 34722, İstanbul, Türkiye

Received: 4 November 2023; Revised: 20 December 2023; Accepted: 20 December 2023

*Corresponding author e-mail: selbi.keskin@giresun.edu.tr

Citation: Keskin, S.; Vural D. *Int. J. Chem. Technol.* 2023, 7 (2), 171-179.

ABSTRACT

Compounds including a triazole skeleton and an imine functional group in their structures have a broad range of applications in drug discovery due to their biological activities. Herein, the novel Schiff bases bearing 1-(*o*-tolyl)-4-(phenoxyethyl)-(1*H*)1,2,3-triazole derivatives were synthesized and the structures of newly synthesized compounds were characterized by FTIR, 1D and 2D NMR and mass spectral data. Computational analysis was performed to optimize the structures of the synthesized compounds with density functional theory (DFT) using the B3LYP method at the 6-311++G(d,p) basis set in the gas phase. The binding affinity values obtained from docking studies of Schiff bases (**2a-2d**) on sterol 14 α -demethylase (CYP51) indicate that compounds **2c** and **2d** have a higher potential as CYP51 inhibitors compared to compounds **2a** and **2b**. It was found that the incorporation of a benzene ring into the structure significantly increased the binding affinity from -9.0 to -11.5 kcal mol⁻¹.

Keywords: Schiff bases, 1,2,3-triazole, molecular docking, sterol 14 α -demethylase.

1. INTRODUCTION

Click chemistry has emerged as a rapid and potent method for the synthesis of heterocyclic compounds with significant biological relevance. The copper-catalyzed 1,3-dipolar azide-alkyne cycloaddition (CuAAC) reaction has been used for the construction of the triazole moiety with high reliability and selectivity.¹⁻³ Compounds based on 1,2,3-triazole have garnered attention for their wide range of biological activities, including antifungal⁴⁻⁷, antileishmanial⁸, antitubercular^{9,10}, antiviral^{11,12}, anti-Alzheimer's¹³ and anticancer^{14,15} activities. Triazole derivatives exhibit robust pharmacological activities, minimizing side effects, reducing multidrug resistances, and showcasing high bioavailability. A number of potent drugs possessing triazole nucleus have been investigated as important medicinal agents, fluconazole (antifungal agents)^{16,17}, mubritinib (antitumor)¹⁸ and rufinamide (antiepileptic)¹⁹ (Figure 1).

Schiff bases, also known as imines or azomethines, constitute an important class of organic compounds and

pharmacophores. These compounds are derived from the condensation reaction between aldehydes or ketones and primary amines in synthetic chemistry. The synthesis, characterization, and structure-activity relationship (SAR) of Schiff bases have been studied worldwide. Notably, the presence of a lone pair of electrons in the sp² hybridized orbital of nitrogen atom in Schiff bases holds considerable chemical and biological importance.^{20,21}

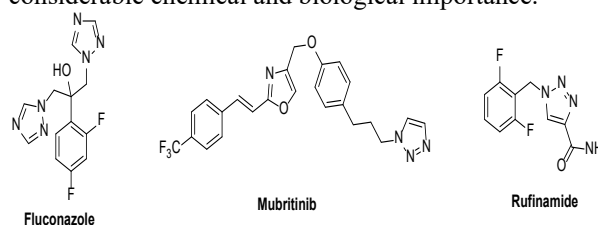


Figure 1. Examples of drugs possessing triazole moiety.

Schiff bases demonstrate a broad range of applications across various fields, including analytical, biological, and inorganic chemistry. Their significance extends to medicine and pharmaceuticals due to their diverse biological effects, making them valuable for activities such as antifungal, antibacterial, antiviral, anticancer,

antioxidant and antimalarial^{22–25} effects. Both triazoles and imines play crucial roles in pharmacology, contributing significantly to various biological activities. As a result, there is growing interest in the synthesis of compounds containing the triazole heterocycle and imine functionality, with ongoing investigations into their biological activities, reflecting the increasing importance of these compounds in scientific research.

Molecular docking is one of the commonly employed techniques in drug discovery to assess the suitability of chemical compounds.^{26,27} Cytochrome P450 (CYP51), also referred as sterol 14 α -demethylase, plays a crucial role in the biosynthesis of ergosterols, a key component of fungal cell membranes. This enzyme is also significant in various other eukaryotes, such as plants and protozoa.^{28–32} Inhibitors of CYP51 bind to its active site, thereby hindering the biosynthesis of ergosterol. These inhibitors are targeted for antifungal drugs, especially for the treatment of fungal infections. CYP51 is widely used for molecular docking because of its well-known 3D structure^{7,30,33} and also used in clinical practices for antifungal medications.^{28,29}

Given the importance and antifungal activities associated with 1,2,3-triazole and Schiff bases, our objective is to synthesize novel derivatives of Schiff bases **2** bearing a triazole moiety and to determine the role of the newly synthesized compounds in the function of Cytochrome P450 applying molecular docking studies. The synthesis involves the condensation reaction between 4-((1-(*o*-tolyl)-1*H*-1,2,3-triazol-4-yl)methoxy)isophthalaldehyde (**1**) and primary amines (Figure 2). The structures of newly synthesized Schiff bases were optimized using density functional theory (DFT) at the B3LYP level with the 6-311++G(d,p) basis set in the gas phase. Additionally, molecular docking studies were conducted for the novel Schiff bases on sterol 14 α -demethylase. This was carried out in order to determine the intermolecular interactions and predict the behavior of these compounds in the binding sites. The comprehensive approach integrates experimental synthesis with computational analyses to provide an understanding of the synthesized compounds' properties and potential biological activities doing molecular docking studies.

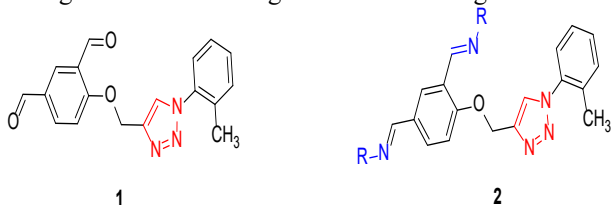


Figure 2. Target structures.

2. MATERIALS AND METHODS

All materials were purchased from commercial sources and utilized without additional purification unless otherwise specified. Reaction progress was monitored by

thin-layer chromatography (TLC) employing a fluorescent indicator visible at 254 nm and 365 nm. Melting points were determined using a Barnstead electrothermal 9200 series digital apparatus with open glass capillaries. Fourier Transform Infrared spectra (400–4000 cm^{-1}) were recorded using a Thermo Scientific Nicolet IS10 ATR FTIR spectrometer with band positions reported in reciprocal centimeters (cm^{-1}). The ^1H NMR (400 MHz) and ^{13}C NMR (100 MHz), along with APT, NOESY, HSQC and HMBC NMR spectra of the compounds, were acquired on a Bruker Ascend 400 (100)-MHz spectrometer using $\text{DMSO-}d_6$ or CDCl_3 as the solvent. Chemical shifts were reported (δ) relative to Me_4Si as the internal standard and coupling constants, J , were reported in hertz (Hz). Mass spectra of the compounds were recorded on an LC/MS High-Resolution Time of Flight (TOF), an Agilent 6530 instrument, at the East Anatolia High Technology Application and Research Center at Atatürk University.

2.1. Experimental

2.1.1. Synthesis of 2-hydroxyisophthalaldehyde (4) and 4-hydroxyisophthalaldehyde (5)³⁴:

Hexamethylenetetramine (4.6 g, 32.7 mmol) and cuprous oxide (2.35 g, 16.4 mmol) were added to a solution of salicylaldehyde (**3**) (2 g, 16.4 mmol) in trifluoroacetic acid (30 mL). The resulting mixture was refluxed for about 5 h. Then, it was cooled to room temperature. A solution of hydrochloric acid (3 N, 30 mL) was added to the mixture and it was stirred for 1 h. The resulting solution was concentrated under reduced pressure. The products (compound **4** and compound **5**) were purified by silica gel column chromatography eluting with hexane: ethyl acetate (7:1).

2.1.1.1. 2-hydroxyisophthalaldehyde (4): White solid. Yield: 11%. ^1H NMR (400 MHz, CDCl_3): δ 11.65 (s, 1H), 10.23 (s, 2H), 7.95 (d, $J = 7.6$ Hz, 2H), 7.12 (t, $J = 7.6$ Hz, 1H). ^{13}C NMR (100 MHz, CDCl_3): δ 192.2, 163.5, 137.7, 123.0, 119.9.

2.1.1.2. 4-hydroxyisophthalaldehyde (5): Yellow solid. Yield: 10%. ^1H NMR (400 MHz, CDCl_3): δ 11.56 (s, 1H), 10.01 (s, 1H), 9.94 (s, 1H), 8.15 (d, $J = 2.0$ Hz, 1H), 8.07 (dd, $J = 8.6, 2.1$ Hz, 1H), 7.14 (d, $J = 8.7$ Hz, 1H). ^{13}C NMR (100 MHz, CDCl_3): δ 196.3, 189.4, 166.4, 137.3, 136.6, 129.3, 120.4, 118.9.

2.1.2. Synthesis of 4-(prop-2-yn-1-yloxy)isophthalaldehyde (6):

4-hydroxyisophthalaldehyde (**5**) (140 mg, 0.93 mmol) was dissolved in 5 mL of dry DMF. Anhydrous K_2CO_3 (193 mg, 1.4 mmol) was then added and stirred at room temperature for 30 minutes. Subsequently, propargyl bromide (80% in toluene) (120 μL , 1.12 mmol) was added at room temperature and stirred overnight. Upon completion of the reaction, ethyl acetate was added to the mixture, and extraction was carried out with water. The

organic phase was washed with saturated brine, followed by drying over Na₂SO₄. The solvent was then removed under vacuum, yielding the reaction product **6** with a 70% yield. ¹H NMR (400 MHz, CDCl₃) δ 10.48 (s, 1H), 9.96 (s, 1H), 8.35 (d, *J* = 2.1 Hz, 1H), 8.13 (dd, *J* = 8.7, 2.1 Hz, 1H), 7.28 (d, *J* = 8.7 Hz, 1H), 4.94 (d, *J* = 2.3 Hz, 2H), 2.64 (t, *J* = 2.3 Hz, 1H). ¹³C NMR (100 MHz, CDCl₃) δ 190.2, 188.4, 163.7, 135.5, 132.0, 130.4, 125.5, 113.8, 77.6, 77.3, 56.9.

2.1.3. Synthesis of 1-azido-2-methylbenzene (7)³⁵: In the reaction flask, *o*-toluidine (1.07 g, 10 mmol) was placed, and a 6 M aqueous solution of HCl (10 mL) was added at 0 °C. Subsequently, a solution of sodium nitrite (1.38 g in 30 mL of water) was added dropwise at 0 °C. After stirring the reaction mixture for 30 minutes, 20 mmol of NaN₃ (1.3 g in 5 mL of water) was added dropwise to the mixture at the same temperature. The resulting mixture was stirred for 2 hours at 0 °C to room temperature and then adjusted to pH = 7. Ethyl acetate was used for extraction, and the organic phase was washed with brine and dried over sodium sulfate. Following the evaporation of the solvent, the brown oily azide **7** was obtained with a quantitative yield and it was used without purification for the next step. ¹H NMR (400 MHz, CDCl₃) δ 7.26 (t, *J* = 7.7 Hz, 1H), 7.19 (d, *J* = 7.4 Hz, 1H), 7.14 (d, *J* = 7.9 Hz, 1H), 7.07 (t, *J* = 7.4 Hz, 1H), 2.24 (s, 3H). The ¹H NMR spectral data are in good agreement with the literature data.³⁶

2.1.4. Synthesis of 4-((1-*o*-tolyl)-1*H*-1,2,3-triazol-4-yl)methoxy)isophthalaldehyde (1): Following the dissolution of the alkyne derivative (**6**) (270 mg, 1.43 mmol) in *t*-BuOH: H₂O (1:1) mixture (20 mL), 1-azido-2-methylbenzene (**7**) (191 mg, 1.43 mmol) was added to the mixture. Then, CuSO₄·5H₂O (357 mg, 1.43 mmol) and *L*-(+)-ascorbic acid (252 mg, 1.43 mmol) were sequentially added. The reaction mixture was stirred at room temperature for 24 h and monitored by TLC. Upon completion of the reaction, the solvent was evaporated and 30 mL of water was added to the residue, followed by extraction with DCM (3x50 mL). The combined organic phases were dried over sodium sulfate and the product (compound **1**) was obtained as a white solid after evaporating the solvent under the vacuum (423 mg, 92% yield). Mp: 164-165 °C. ¹H NMR (400 MHz, CDCl₃): δ 10.49 (s, 1H), 9.98 (s, 1H), 8.36 (d, *J* = 2.1 Hz, 1H), 8.16 (dd, *J* = 8.7, 2.1 Hz, 1H), 7.91 (s, 1H), 7.47 – 7.42 (m, 2H), 7.39 (d, *J* = 7.7 Hz, 1H), 7.37 – 7.32 (m, 2H), 5.55 (s, 2H), 2.22 (s, 3H). ¹³C NMR (100 MHz, CDCl₃): δ 190.2, 188.5, 164.5, 136.2, 136.0, 133.7, 132.1, 131.7, 130.4, 130.2, 127.1, 126.1, 125.3, 125.0, 124.9, 113.8, 63.0, 18.0. IR (ATR, cm⁻¹) 3140, 2845, 1683, 1682, 1601, 1576, 1491, 1429, 1381, 1260, 1162, 1094, 822, 754. HRMS-TOF [M+H]⁺ Calculated for C₁₈H₁₅N₃O₃ 321.11134, found: 321.11098.

2.1.5. Synthesis of methyl substituted (compound 2a) and ethyl substituted (compound 2b) imines: To a

stirring solution of dialdehyde **1** (50 mg, 0.16 mmol) in 5 mL of dichloromethane at room temperature, 40% aqueous solution of methyl amine (100 μL, 1.16 mmol) or 70% aqueous solution of ethyl amine (98 μL, 1.23 mmol) was added. The reaction mixture was stirred at room temperature overnight. Subsequently, the resulting solution was dried over Na₂SO₄ and the solvent was evaporated under reduced pressure yielding the corresponding imine (**2a** or **2b**).

2.1.5.1. (1*E*,1'*E*)-1,1'-(4-((1-*o*-tolyl)-1*H*-1,2,3-triazol-4-yl)methoxy)-1,3-phenylene)bis(*N*-methylmethanimine (2a)): Yellowish solid with a 96% yield. Mp: 132-133 °C. ¹H NMR (400 MHz, CDCl₃): δ 8.64 (br s, 1H), 8.18 (br s, 1H), 8.10 (s, 1H), 7.83 (d, *J* = 7.2 Hz, 1H), 7.79 (s, 1H), 7.41 – 7.35 (m, 1H), 7.33 – 7.25 (m, 3H), 7.11 (d, *J* = 8.6 Hz, 1H), 5.36 (s, 2H), 3.45 (s, 3H), 3.42 (s, 3H), 2.16 (s, 3H). ¹³C NMR (100 MHz, CDCl₃): δ 161.3, 158.7, 157.6, 143.3, 136.3, 133.6 (2C), 131.6, 130.04, 129.97, 128.3, 126.9, 126.0, 125.1, 124.5, 113.0, 62.5, 48.5, 48.1, 17.9. IR (ATR, cm⁻¹) 3138, 2937, 2882, 1646, 1600, 1493, 1456, 1367, 1244, 1107, 1044, 998, 960, 814, 758. HRMS-TOF [M+H]⁺ Calculated for C₂₀H₂₁N₅O 347.17461, found: 347.17386.

2.1.5.2. (1*E*,1'*E*)-1,1'-(4-((1-*o*-tolyl)-1*H*-1,2,3-triazol-4-yl)methoxy)-1,3-phenylene)bis(*N*-ethylmethanimine (2b)): Yellowish solid with a 98% yield. Mp: 123-124 °C. ¹H NMR (400 MHz, CDCl₃): δ 8.69 (br s, 1H), 8.24 (br s, 1H), 8.18 (s, 1H), 7.88 (d, *J* = 8.5 Hz, 1H), 7.79 (s, 1H), 7.44 – 7.39 (m, 1H), 7.39 – 7.30 (m, 3H), 7.14 (d, *J* = 8.6 Hz, 1H), 5.40 (s, 2H), 3.65 – 3.56 (m, 4H), 2.20 (s, 3H), 1.31 – 1.17 (m, 6H). ¹³C NMR (100 MHz, CDCl₃): δ 159.5, 158.9, 155.8, 143.5, 136.4, 133.8, 131.7, 130.3, 130.2 (2C), 128.6, 127.0, 126.1, 125.3, 124.5, 112.9, 62.7, 56.3, 55.9, 18.0, 16.5 (2C). IR (ATR, cm⁻¹) 3112, 3065, 2970, 2849, 1640, 1604, 1494, 1469, 1326, 1257, 1242, 1168, 1027, 965, 832, 764. HRMS-TOF [M+H]⁺ Calculated for C₂₂H₂₅N₅O 375.20591, found: 375.20554.

2.1.6. Synthesis of benzyl substituted (compound 2c) and 4-dimethylaminophenyl substituted (compound 2d) imines: To the stirring solution of dialdehyde **1** (40 mg, 0.13 mmol) in 5 mL of hot ethanol, benzyl amine (28 μL, 0.26 mmol) or *N,N*-dimethyl-*p*-phenylenediamine (**8**) (35 mg, 0.13 mmol) was added at 70 °C and the resulting mixture was refluxed overnight. Then, the reaction mixture was cooled to room temperature and the solvent was evaporated under reduced pressure to obtain the corresponding product (**2c** or **2d**).

2.1.6.1. (1*E*,1'*E*)-1,1'-(4-((1-*o*-tolyl)-1*H*-1,2,3-triazol-4-yl)methoxy)-1,3-phenylene)bis(*N*-benzylmethanimine (2c)): Brownish oily compound with a 95% yield. ¹H NMR (400 MHz, DMSO): δ 8.78 (br s, 1H), 8.65 (s, 1H), 8.46 (br s, 1H), 8.28 (br s, 1H), 7.86 (d, *J* = 7.1 Hz, 1H), 7.49 – 7.38 (m, 6H), 7.32 – 7.25 (m, 7H), 7.25 – 7.17 (m, 2H), 5.43 (s, 2H), 4.75 (s, 2H),

4.70 (s, 2H), 2.12 (s, 3H). ^{13}C NMR (100 MHz, DMSO): δ 160.9, 159.0, 156.5, 142.6, 139.7, 139.6, 136.2, 133.1, 131.8, 131.4, 129.9, 129.3, 128.4 (4C), 128.0 (2C), 127.9 (2C), 127.0, 126.8 (2C), 126.6, 126.2, 126.1, 124.5, 113.7, 64.4, 64.0, 62.2, 17.4. IR (ATR, cm^{-1}) 3061, 3027, 2872, 1638, 1600, 1494, 1452, 1370, 1245, 1112, 1023, 992, 818, 762, 697. HRMS-TOF $[\text{M}+\text{H}]^+$ Calculated for $\text{C}_{32}\text{H}_{29}\text{N}_5\text{O}$ 499.23721, found: 499.23885.

2.1.6.2. 4,4'-(((1E,1'E)-(4-((1-*o*-tolyl)-1*H*-1,2,3-triazol-4-yl)methoxy)-1,3-phenylene)bis(methanylylidene))bis(azanylyl-idene))bis(*N,N*-dimethylaniline) (2d): Brownish solid with a 97% yield. Mp: 77-78 °C. ^1H NMR (400 MHz, CDCl_3): δ 8.95 (br s, 1H), 8.54 (s, 1H), 8.52 (br s, 1H), 8.11 (d, $J = 8.2$ Hz, 1H), 7.80 (s, 1H), 7.46 – 7.31 (m, 5H), 7.29 – 7.26 (m, 2H), 7.25 – 7.20 (m, 2H), 6.76 (t, $J = 8.6$ Hz, 4H), 5.48 (s, 2H), 2.984 (s, 6H), 2.976 (s, 6H), 2.21 (s, 3H). ^{13}C NMR (100 MHz, CDCl_3): δ 159.4, 155.0, 151.2, 149.6, 149.5, 143.4, 141.4, 140.9, 136.3, 133.7, 131.6, 130.7, 130.6, 130.0, 128.8, 126.9, 126.1, 126.0, 124.6, 122.5 (2C), 122.3 (2C), 113.1, 113.0 (2C), 112.9 (2C), 62.7, 40.82 (2C), 40.78 (2C), 18.0. IR (ATR, cm^{-1}) 2980, 2850, 1605, 1604, 1511, 1442, 1348, 1260, 1163, 1100, 1043, 944, 814, 760. HRMS-TOF $[\text{M}+\text{H}]^+$ Calculated for $\text{C}_{34}\text{H}_{35}\text{N}_7\text{O}$ 557.29031, found: 557.29105.

2.2. Computational Procedures

Geometry optimization studies of Schiff bases (compounds **2a-2d**) were performed using the Density Functional Theory (DFT) method in Gaussian 09W³⁷ at 298.15 Kelvin and 1 atm. The functional and basis set for the DFT method were chosen as B3LYP and 6-311++G(d,p), respectively.^{38,39} The calculated optimized structures of the Schiff bases were generated using GaussView5.0.⁴⁰

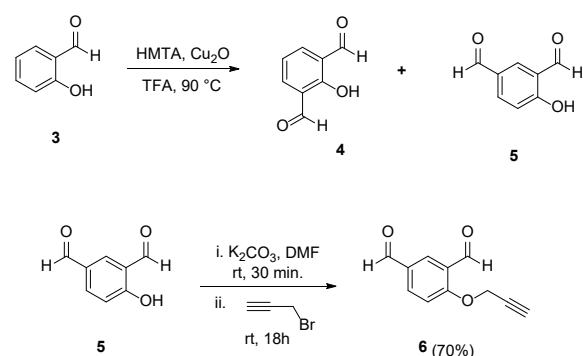
Molecular docking analysis was performed using the popular docking program AutoDock Vina 1.1.2.⁴¹ The three-dimensional structure of sterol 14 α -demethylase (CYP51) (PDB ID:5YZ1) was obtained from the Protein Data Bank⁴² (Figure 5). Receptor data were processed using AutoDockTools (ADT) 1.5.6⁴³ and the natural ligands, attached to sterol 14 α -demethylase (CYP51), and water molecules were removed. Nonpolar hydrogen atoms were subsequently added. The protein (chain A) file was saved in AutoDock pdbqt format and made ready for docking. Similarly, the synthesized Schiff bases chosen as ligands were prepared using AutoDockTools. The search box size was set to 50Åx50Åx50Å with a grid spacing of 0.375 Å at the center position (70.555, 66.424, 3.943). The exhaustiveness was set to 8. The interactions between Schiff bases (**2a-2d**) and CYP51 were analyzed using Discovery Studio Visualizer.⁴⁴

3. RESULTS AND DISCUSSION

3.1 Chemistry

Our initial aim was to construct (1*H*)-1,2,3-triazole moiety. To achieve this, we employed the copper-catalyzed 1,3-dipolar azide-alkyne cycloaddition (CuAAC) reaction between an alkyne and an azide. Firstly, compound **6** having propargyl group adjacent to the oxygen atom was synthesized starting from commercially available salicylaldehyde (**3**). We followed the synthetic strategy outlined in Scheme 1. The process involved the reaction of salicylaldehyde (**3**) with hexamethylenetetramine (HMTA) in the presence of Cu_2O in trifluoroacetic acid (TFA) following a literature procedure.³⁴ After purifying the corresponding aldehyde **5**, it was treated with propargyl bromide in the presence of K_2CO_3 , resulting in the synthesis of compound **6** with a yield of 70%⁴⁵ (Scheme 1). The NMR spectra belonging to these compounds are seen in Figure S1-S6 in the Supporting Information (SI).

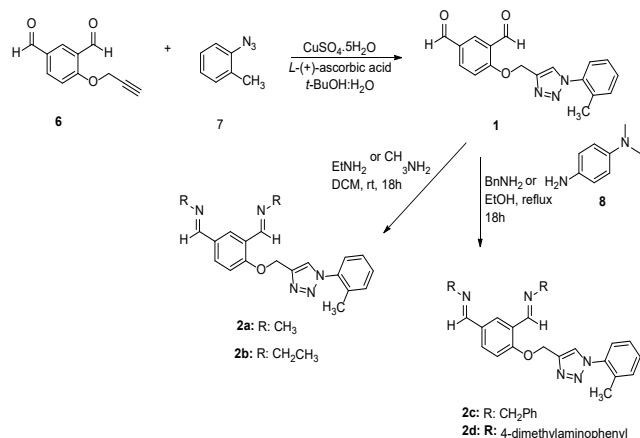
On the other hand, azide **7** was prepared by initiating the diazotization of *o*-toluidine using HCl/NaNO_2 , followed by treating the resulting diazonium salt with NaN_3 . The product was used in the next step without further purification. The ^1H NMR data of compound **7** (Figure S7) was found to be in accordance with the literature data³⁶. After obtaining the precursors for the CuAAC reaction (compound **6** and compound **7**), they were reacted in the presence of $\text{CuSO}_4 \cdot 5\text{H}_2\text{O}$ and *L*-(+)-ascorbic acid in *t*-BuOH: H_2O (1:1) at room temperature by stirring overnight inspired by a procedure previously applied by our group.⁴⁶ The reaction product **1** was isolated and characterized using suitable spectroscopic techniques (Scheme 2).



Scheme 1. Synthesis of starting material.

Compound **1** is a (1*H*)-1,2,3-triazole derivative featuring two aldehyde functional groups adjacent to the benzene ring. Our subsequent aim was to convert these aldehyde functionalities into imines through a condensation reaction, followed by molecular docking studies to analyze their potential biological activities. To obtain novel Schiff bases, we employed two different synthetic strategies inspired by literature procedures.^{47,48} Compound **1** was treated with methyl amine solution in dichloromethane (DCM) at room temperature, yielding the corresponding imine **2a**. The formation of the ethyl-substituted imine derivative **2b** was also carried out by treating an ethylamine solution with compound **1** in DCM at room temperature. Additionally, a condensation

reaction between two equivalents of benzyl amine and compound **1** in ethanol at reflux temperature resulted in the incorporation of two benzyl groups into the structure, producing the corresponding imine **2c**. The same reaction conditions were also applied using aromatic amine (*N,N*-dimethyl-*p*-phenylenediamine (**8**)), leading to the expected Schiff base product **2d** obtained with 97% yield. All novel products (**1** and **2a-2d**) were characterized with the help of ^1H NMR, ^{13}C NMR, FTIR and HRMS data.



Scheme 2. Synthesis of target molecules (compound **1** and **2a-2d**).

3.2 Spectroscopic characterization

Nuclear Magnetic Resonance (NMR) Spectroscopy, HRMS, FTIR were used for the characterization of the compounds. ^1H NMR and ^{13}C NMR spectra of all synthesized compounds and 2D NMR spectra of compound **2a** are given in Figures S1-S20. In the ^1H NMR spectrum of compound **1** (Figure S8), singlets at 7.91 ppm, 5.55 ppm and 2.22 ppm confirm the formation of the desired product. The singlet at 7.91 corresponds to the triazolyl proton. The other singlet signal at 2.22 ppm belongs to the CH₃ protons bonded to the benzene ring. While methylene protons in compound **6** resonate as a doublet with the coupling constant of 2.3 Hz, methylene protons in the ^1H NMR spectrum of compound **1** give a resonance signal at 5.55 ppm as a singlet. Furthermore, no triplet signal from acetylenic hydrogen was observed in the ^1H NMR spectrum of the product. During the structural analysis of Schiff bases (**2a-2d**), the disappearance of singlets (at 10.49 ppm and 9.98 ppm in the ^1H NMR spectrum of compound **1**) corresponding to aldehyde functionalities and the appearance of resonance signals of H-C=N protons (ranging from 8.95 to 8.18 ppm) in the ^1H NMR spectra provide evidence for the formation of Schiff bases. For a detailed structural analysis, 2D NMR spectra of imine **2a** were examined. In the ^1H -NMR spectrum, two broad singlets belonging to imine hydrogens, H7 and H23, were observed at 8.64 ppm and 8.18 ppm. Assignments of these hydrogens were made with the assistance of HSQC and HMBC spectra

(Figures S13 - S14). It was found that the imine hydrogen resonating at 8.64 ppm correlates with the carbon signal at 157.6 ppm while the other imine hydrogen correlates with the carbon resonating at 161.3 ppm in the HSQC spectrum. In addition, the HMBC spectrum reveals the detailed correlations of the imine carbons of the compound **2a**. It was determined that the imine carbon at 161.3 ppm is C3, the hydrogen at 8.18 ppm is H7, the resonance signal at 8.64 ppm in the ^1H NMR spectrum belongs to H23, and the signal at 157.6 ppm belongs to C17. To identify the methyl hydrogens adjacent to imine nitrogen atoms, the correlations of imine carbon atoms were examined. It was observed that C3 correlates with a singlet signal at 3.42 ppm (H4, H5, H6) while C17 correlates with a singlet signal at 3.45 ppm (H20, H21, H22) over 3 bonds in the HMBC spectrum. In the ^1H -NMR spectrum, the resonance signal at 7.79 ppm as a singlet belongs to H33 which is bonded to C30 (at 124.5 ppm). This CH carbon gives a correlation with the CH₂ proton in the HMBC spectrum while H33 correlates with C28 over 2 bonds.

Additionally, a NOESY NMR experiment of compound **2a** was conducted to identify the stereochemistry of the Schiff bases. In the NOESY spectrum of compound **2a** shown in Figure 3, NOE signals were observed between imine NH protons at 8.64 ppm and 8.18 ppm and the methyl protons resonating at 3.45 ppm and 3.42 ppm respectively. This provides evidence that it is the *E* isomer, and it is expected that this signal would not be observed in the *Z*-isomer.

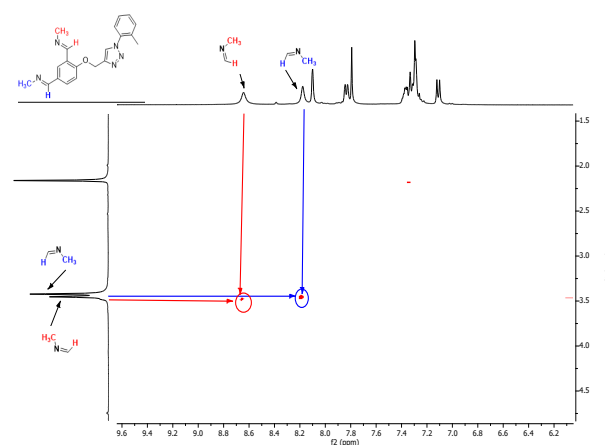


Figure 3. NOESY spectrum of compound **2a**.

In addition to NMR analysis, an IR analysis was performed. In the IR spectrum of compound **1**, bands at 3140 cm^{-1} and 1381 cm^{-1} confirm the formation of the triazole skeleton due to the C-H stretching and C-N stretching in the triazole. The absorption bands of the C=O group of aldehyde functionalities at 1682 cm^{-1} and 1683 cm^{-1} were observed. In the IR spectra of Schiff bases (**2a-2d**), the characteristic absorption bands at 1600-1646 cm^{-1} indicate the formation of the imine functional group due to C = N stretching vibrations. Additionally, C-H stretching vibrations and C-N

stretching vibrations of the triazole ring are in the region of 3000-3150 cm^{-1} and 1300-1399 cm^{-1} , respectively.

3.3 Optimization and Molecular Docking

The optimized structures of the Schiff bases, **2a** and **2c**, generated using GaussView5.0, are displayed in Figure 4 (see Figure S21 for other compounds **2b** and **2d**). The calculated structural parameters such as bond lengths, bond angles and dihedral angles, and Z-matrices for all compounds (**2a-2d**), are in Table S1-S8. The benzene rings adjacent to the oxygen atom, 1,2,3-triazole rings and the intersection plane between them is the common skeleton of these compounds. To investigate the optimized geometrical structure with the minimum potential energy surface, the orientation of the benzene and 1,2,3-triazole rings with respect to the intersection plane has been investigated. For compound **2c**, the dihedral angles, C11-C12-O21-C22, C12-O21-C22-C25 and O21-C22-C25-C27, are 178.51°, -177.05° and 2.61°, respectively. These results indicate that molecules are not planar, which is consistent with molecules having sp^2 and sp^3 hybridized atoms.

The C-C-C angles in the benzene ring for both compounds (**2a** and **2c**) vary between 118° and 123°, slightly distorted from the typical hexagonal angle of 120°, while other angles in 1,2,3-triazole, such as C-N-N, N-N-N and C-C-N, are found in the range of 104°-110°. In the common skeleton of compounds (benzene adjacent to oxygen atom and 1,2,3-triazole), C-C bond lengths vary between 1.37 Å and 1.41 Å while N-N bond lengths are measured as 1.30 Å for double bond and 1.35 Å for single bond. The C-N bond lengths in 1,2,3-triazole

ring are found 1.36 Å. These values are in good agreement with the values in literature.⁴⁹

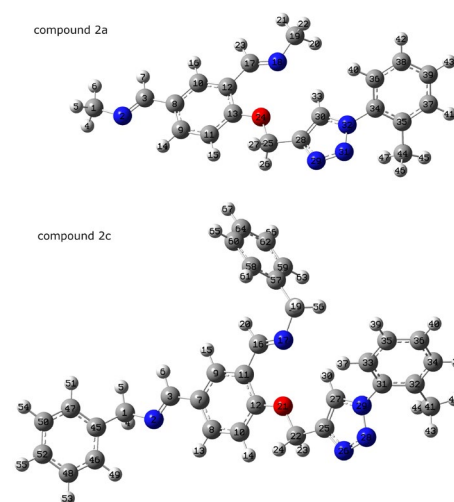


Figure 4. Optimized molecular structure of compounds **2a** and **2c** obtained using GaussView5.0.

Molecular docking was performed to predict the interaction between compounds **2a-2d** with CYP51 (PDB ID:5TZ1) using AutoDock Vina. The binding affinities for the most favorable binding modes of all compounds (**2a-2d**) are presented in Table 1. DS Visualizer was used to generate two- and three-dimensional docking representations of all compounds, but only compounds **2a** and **2c** are displayed in Figure 5. The docking representations of other compounds (**2b** and **2d**) are in Figure S22. It has been noted in Table 1 that compounds **2c** and **2d** demonstrate greater affinities for binding compared to compounds **2a** and **2b**.

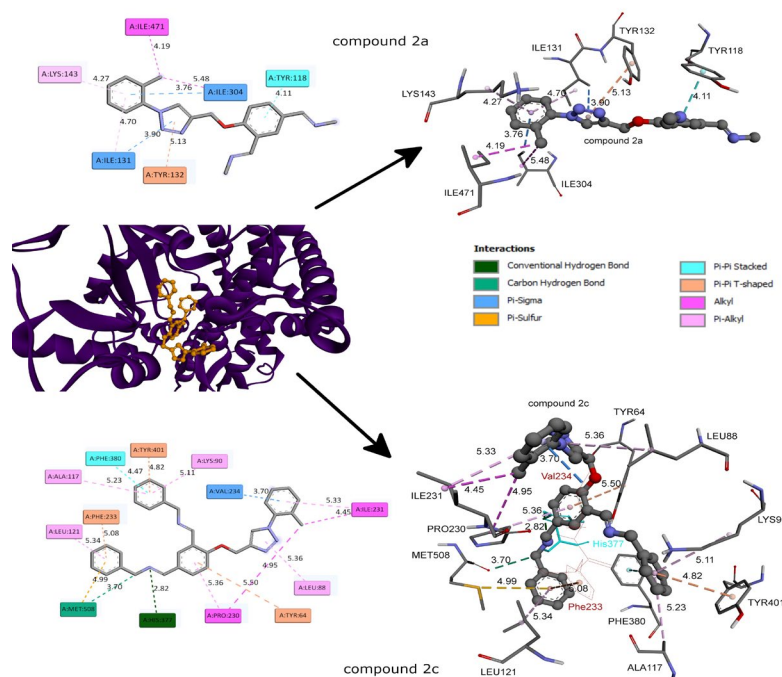


Figure 5. Binding interactions of compounds **2a** and **2c** in active site of CYP51 (PDB ID: 5TZ1) with binding affinities of -9.0 and -11.5 kcal mol^{-1} .

Table 1. Best binding scores of compounds.

| Compound | Affinity (kcal/mol) | Distance from best RMSD (Å) |
|-----------|---------------------|-----------------------------|
| 2a | -9.0 | 0.0 |
| 2b | -9.1 | 0.0 |
| 2c | -11.5 | 0.0 |
| 2d | -11.3 | 0.0 |

Molecular docking results also reveal interactions between amino acid residues on CYP51 and functional groups in the compounds **2a-2d**. Here, we observed two types of interactions; hydrophilic and hydrophobic. These interactions serve as an “anchor”, guiding the 3D orientation of the compounds **2a-2d** in the active site of CYP51 (Figures 5 and S22). The binding affinities of compounds **2a-2d** are in the range from -9.0 to -11.5 kcal mol⁻¹ (Table 1). The binding affinity values indicate that interaction between compound **2c** and CYP51 is stronger than that between the compound **2a** and CYP51.

To explain the binding affinity difference between compounds, it is important to compare the interactions of these compounds with CYP51. The π - π stacked, π - σ , π - π T-shaped, alkyl-alkyl and π -alkyl hydrophobic interactions were observed between all compounds and CYP51 (Table 2, Figures 5 and S22). The hydrophobic interaction distance for compounds **2a** and **2c** varies in the range of 4-6 Å. However, it is notable that the quantity of hydrophobic interactions, particularly π - π T-shaped and π -alkyl interactions, for compound **2c** is greater than for compound **2a**.

Table 2. Interactions between compounds **2a** and **2c** with CYP51.

| | Compound 2a | Compound 2c |
|----------------------------|--|--|
| Conventional Hydrogen Bond | | HIS377: H...N: Ligand, 2.82 Å |
| Carbon Hydrogen Bond | | Ligand: CH...O: MET508, 3.70 Å |
| Pi-Sigma | ILE131: CH...Pi-orbital: Ligand, 3.90 Å ILE304: CH...Pi-orbital: Ligand, 3.76 Å | VAL234: CH...Pi-orbital: Ligand, 3.70 Å |
| Pi-Sulfur | | MET508: S...Pi-orbital: Ligand, 4.99 Å |
| Pi-Pi Stacked | Ligand: Pi-orbital...Pi-orbital: TYR118, 4.11 Å | PHE380: Pi-orbital...Pi-orbital: Ligand, 4.47 Å |
| Pi-Pi T-shaped | Ligand: Pi-orbital...Pi-orbital: TYR132, 5.13 Å | TYR64: Pi-orbital...Pi-orbital: Ligand, 5.50 Å PHE233: Pi-orbital...Pi-orbital: Ligand, 5.08 Å TYR401: Pi-orbital...Pi-orbital: Ligand, 4.82 Å |
| Alkyl-Alkyl | Ligand...ILE304, 5.48 Å Ligand...ILE471, 4.19 Å | Ligand...PRO230, 4.95 Å Ligand...ILE231, 4.45 Å |
| Pi-Alkyl | Ligand...ILE131, 4.70 Å Ligand...LYS143, 4.27 Å | Ligand...PRO230, 5.36 Å Ligand...LEU88, 5.36 Å Ligand...ILE231, 5.33 Å Ligand...LYS90, 5.11 Å Ligand...ALA117, 5.23 Å Ligand...LEU121, 5.34 Å |

Unlike compound **2a**, compound **2c** has additional two hydrogen bond interactions and one π -sulfur interaction with target protein. Hydrogen bond interactions between compound **2c** and CYP51; (i) (O...CH) form interaction is between O atom of residue MET508 and CH₂ bonded to nitrogen atom of imine functional group with 3.7 Å, and (ii) (H...N) form interaction is between H atom of residue HIS377 and N=C with 2.82 Å. Furthermore, the π -electron cloud over the aromatic benzene ring of benzyl group of compound **2c** interacts with the sulfur atom in residue MET508 on CYP51. This π -sulfur interaction distance is around 5 Å.

4. CONCLUSIONS

The new derivatives of Schiff bases bearing 1-(*o*-tolyl)-4-(phenoxyethyl)-(1*H*)-1,2,3-triazole **2a-d** were synthesized through CuAAC by reacting 4-((1-(*o*-tolyl)-1*H*-1,2,3-triazol-4-yl)methoxy)isophthalaldehyde (**1**) with primary amines. Characterization studies were conducted using appropriate spectroscopic techniques. The geometry of these Schiff bases, including bond lengths, angles, and torsional angles, was characterized using computational methods. These novel imine derivatives have the potential to exhibit high antifungal

activity due to the significant triazole ring and imine functionalities in their structures. Consequently, we investigated the interaction between compounds **2a-2d** and sterol 14 α -demethylase (CYP51) through molecular docking studies. The binding affinities of the imines (**2a-2d**) were determined as -9.0, -9.1, -11.5, and 11.3 kcal mol⁻¹, respectively. These results indicate that the incorporation of an additional aromatic benzene ring into the structure enhances their potential to be an inhibitor for CYP51 due to the additional hydrophobic and hydrogen bond interactions between compound **2c** and sterol 14 α -demethylase (CYP51). We expect that this study provides encouraging results for further biological activity studies on Schiff bases bearing (1,2,3)-triazole derivatives.

Conflict of interests

The authors declare that there is no conflict of interest with any person, institute, or company.

REFERENCES

- Bock, V. D.; Hiemstra, H.; Van Maarseveen, J. H. *European J. Org. Chem.* **2006**, 51-68.
- Meldal, M.; Tornøe, C. W. *Chem. Rev.* **2008**, *108*, 2952-3015.
- Hein, J. E.; Fokin, V. V. *Chem. Soc. Rev.* **2010**, *39* (4), 1302-1315.
- Lima-Neto, R. G.; Cavalcante, N. N. M.; Srivastava, R. M.; Mendonça, F. J. B.; Wanderley, A. G.; Neves, R. P.; Dos Anjos, J. V. *Molecules* **2012**, *17*, 5882-5892.
- Dai, Z.-C.; Chen, Y.-F.; Zhang, M.; Li, S.-K.; Yang, T.-T.; Shen, L.; Wang, J.-X.; Qian, S.-S.; Zhu, H.-L.; Ye, Y.-H. *Org. Biomol. Chem.* **2015**, *13*, 477-486.
- Aher, N. G.; Pore, V. S.; Mishra, N. N.; Kumar, A.; Shukla, P. K.; Sharma, A.; Bhat, M. K. *Bioorganic Med. Chem. Lett.* **2009**, *19*, 759-763.
- Shaikh, M. H.; Subhedar, D. D.; Khedkar, V. M.; Jha, P. C.; Khan, F. A. K.; Sangshetti, J. N.; Shingate, B. B. *Chinese Chem. Lett.* **2016**, *27*, 1058-1063.
- Teixeira, R. R.; Gazolla, P. A. R.; da Silva, A. M.; Borsodi, M. P. G.; Bergmann, B. R.; Ferreira, R. S.; Vaz, B. G.; Vasconcelos, G. A.; Lima, W. P. *Eur. J. Med. Chem.* **2018**, *146*, 274-286.
- Surineni, G.; Yogeewari, P.; Sriram, D.; Kantevari, S. *Med. Chem. Res.* **2015**, *24*, 1298-1309.
- Boechat, N.; Ferreira, V. F.; Ferreira, S. B.; Ferreira, M. D. L. G.; Da Silva, F. D. C.; Bastos, M. M.; Costa, M. D. S.; Lourenço, M. C. S.; Pinto, A. C.; Krettli, A. U.; Aguiar, A. C.; Teixeira, B. M.; Da Silva, N. V.; Martins, P. R. C.; Bezerra, F. A. F. M.; Camilo, A. L. S.; Da Silva, G. P.; Costa, C. C. P. *J. Med. Chem.* **2011**, *54*, 5988-5999.
- Viegas, D. J.; da Silva, V. D.; Buarque, C. D.; Bloom, D. C.; Abreu, P. A. *Antivir. Ther.* **2020**, *25*, 399-410.
- Jordão, A. K.; Afonso, P. P.; Ferreira, V. F.; de Souza, M. C. B. V.; Almeida, M. C. B.; Beltrame, C. O.; Paiva, D. P.; Wardell, S. M. S. V.; Wardell, J. L.; Tiekink, E. R. T.; Damaso, C. R.; Cunha, A. C. *Eur. J. Med. Chem.* **2009**, *44*, 3777-3783.
- Monceaux, C. J.; Hirata-Fukae, C.; Lam, P. C. H.; Totrov, M. M.; Matsuoka, Y.; Carlier, P. R. *Bioorganic Med. Chem. Lett.* **2011**, *21*, 3992-3996.
- Dong, H. R.; Wu, J. G. *Heterocycl. Commun.* **2018**, *24*, 109-112.
- Gaddameedi, J. D.; Yedla, P.; Kuchukulla, R. R.; Chavva, K.; Pillalamarri, S. R.; Gautham, S. K.; Chityal, G. K.; Banda, N. J. *Heterocycl. Chem.* **2017**, *54*, 194-205.
- Vincent-Ballereau, F. N.; Patey, O. N.; Lafaix, C. *Pharm. Weekbl. Sci. Ed.* **1991**, *13*, 45-57.
- Pasko, M. T.; Piscitelli, S. C.; Van Slooten, A. D. *Ann. Pharmacother.* **1990**, *24*, 860-867.
- Dong, J.; Zhu, D.; Chen, M.; Wang, T.; Gao, Y.; Liu, W. *Thorac. Cancer* **2022**, *13*, 1513-1524.
- Wheless, J. W.; Vazques, B. V. *Curr. Rev. Clin. Sci.* **2010**, *10*, 1-6.
- Kabak, M.; Elmali, A.; Elerman, Y. *J. Mol. Struct.* **1999**, *477*, 151-158.
- Patai, S. The Chemistry of the Carbon-Nitrogen Double Bond. In *Interscience*; New York, 1970; pp 149-180.
- Raju, S. K.; Settu, A.; Thiyagarajan, A.; Rama, D.; Sekar, P.; Kumar, S. *GSC Biol. Pharm. Sci.* **2022**, *21*, 203-215.
- Dzeikala, A.; Sykula, A. *J. Pharm. Pharmacol.* **2018**, *6*, 989-1009.
- Arulmurugan, S.; Kavitha, H. P.; Venkatraman, B. R. *Rasayan J. Chem.* **2010**, *3*, 385-410.
- Da Silva, C. M.; Da Silva, D. L.; Modolo, L. V.; Alves, R. B.; De Resende, M. A.; Martins, C. V. B.; De Fátima, Â. *J. Adv. Res.* **2011**, *2*, 1-8.
- Almutairi, M. S.; Zakaria, A. S.; Ignasius, P. P.; Al-Wabli, R. I.; Joe, I. H.; Attia, M. I. *J. Mol. Struct.* **2018**, *1153*, 333-345.
- Ali, M. T.; Blicharska, N.; Shilpi, J. A.; Seidel, V. *Sci. Rep.* **2018**, *8*:12238, 1-8.
- Lepesheva, G. I.; Waterman, M. R. *Biochim. Biophys. Acta* **2007**, *1770*, 467-477.

29. Lepesheva, G. I.; Waterman, M. R. *Curr. Top. Med. Chem.* **2011**, *11*, 2060-2071.
30. Hargrove, T. Y.; Wawrzak, Z.; Liu, J.; Waterman, M. R.; Nes, W. D.; Lepesheva, G. I. *J. Lipid Res.* **2012**, *53*, 311-320.
31. Fan, J.; Urban, M.; Parker, J. E.; Brewer, H. C.; Kelly, S. L.; Hammond-Kosack, K. E.; Fraaije, B. A.; Liu, X.; Cools, H. J. *New Phytol.* **2013**, *198*, 821-835.
32. Friggeri, L.; Hargrove, T. Y.; Wawrzak, Z.; Guengerich, F. P.; Lepesheva, G. I. *J. Med. Chem.* **2019**, *62*, 10391-10401.
33. Kumar, A.; Lal, K.; Poonia, N.; Kumar, A.; Kumar, A. *Res. Chem. Intermed.* **2022**, *48*, 2933-2948.
34. Fu, X. W.; Pu, W. C.; Zhang, G. L.; Wang, C. *Res. Chem. Intermed.* **2015**, *41*, 8147-8158.
35. Awolade, P.; Cele, N.; Kerru, N.; Singh, P. *Mol. Divers.* **2021**, *25*, 2201-2218.
36. Xie, S.; Zhang, Y.; Ramström, O.; Yan, M. *Chem. Sci.* **2016**, *7*, 713-718.
37. Frisch, M. J.; Trucks, G. W.; Schlegel, H. B.; G. E. Scuseria, et al. Gaussian 09, Revision C.01. *Gaussian Inc. Wallingford, CT* **2009**.
38. Becke, A. D. *J. Chem. Phys.* **1993**, *98*, 5648-5652.
39. Lee, C.; Yang, W.; Parr, R. G. *Phys. Rev. B* **1988**, *37*, 785-789.
40. Dennington, R.; Keith, T.; Millam, J. GaussView, Version 5. Semichem Inc. *Shawnee Mission* **2009**.
41. Trott, O.; Olson, A. J. *J. Comput. Chem.* **2010**, *31*, 455-461.
42. Berman, H. M.; Westbrook, J.; Feng, Z.; Gilliland, G.; Bhat, T. N.; Weissig, H.; Shindyalov, I. N.; Bourne, P. E. *Nucleic Acids Res.* **2000**, *28*, 235-242.
43. Morris, G. M.; Huey, R.; Lindstrom, W.; Sanner, M. F.; Belew, R. K.; Goodsell, D. S.; Olson, A. J. *J. Comput. Chem.* **2009**, *30*, 2785-2791.
44. *BIOVIA, Dassault Systemes, Discovery Studio Modeling Environment, Release 2017, San Diego*; 2016.
45. Keskin, S.; Balci, M. *Org. Lett.* **2015**, *17*, 964-967.
46. Keskin, S. *ChemistrySelect* **2023**, *8*, e202302133 (1-7).
47. Bisht, R.; Chattopadhyay, B. *J. Am. Chem. Soc.* **2016**, *138* (1), 84-87.
48. Yeap, G. Y.; Heng, B. T. *J. Chem. Sci.* **2014**, *126* (1), 247-254.
49. Peng, W.; Zhu, S. *J. Fluor. Chem.* **2002**, *116*, 81-86.